

## [27]全国共同利用研究成果報告

<https://hdl.handle.net/2324/7431319>

---

出版情報：全国共同利用研究成果報告. 27, pp.1-, 2024-03. Research Institute for Applied Mechanics, Kyushu University

バージョン：

権利関係：



## 特定研究1【国際】

回転成層流体における波動現象の多角的理解

Multidisciplinary study of wave dynamics in rotating stratified fluids

統括責任者：大貫 陽平（地球環境力学分野）

地球海洋や惑星大気には、天体の自転に起因したコリオリ力や重力成層した流体に働く浮力を復元力した多様な波動現象が存在します。これらの波動は、流れ場との相互作用や境界における反射・散乱を繰り返しながらエネルギーや運動量を運ぶことで、環境システムにおいて重要な役割を果たしています。

本特定研究では、海洋・大気における波動現象への理解を飛躍的に高め、全球数値モデルの精度向上や次世代観測衛星のデータ分析に資することを目指し、基礎流体物理的な研究を推進します。特に大型回転水槽実験やトポロジー理論を強みとした欧州グループとの連携を強化し、実験・理論・シミュレーションを柱とした多角的な研究アプローチを展開します。

## 金星大気波動の解析

慶應義塾大学法学部 杉本憲彦

**目的:** 金星は、その固体部分が半径や重力加速度などの点で地球とよく似ているため、地球の兄弟星と呼ばれる。しかし、その自転周期は非常に遅く、約 243 日にもなる。またその大気部分は、二酸化炭素を主成分とし、約 92 気圧にも達しており、地球と大きく異なる。高度 45-70km 付近には、厚い雲層が存在し、大気循環の全貌は解明されていない。特に大気全体が自転を追い越す方向に約 4 日周期(～100m/s)で回転するスーパーローテーションの成因解明は、地球流体力学的にも興味深い研究テーマである。2015 年には、我が国の金星探査機「あかつき」が金星軌道への再投入に成功し、様々な時空間スケールの波動が観測されたが、これらの波動の 3 次元構造や働き、理論的解釈は十分に研究されていない。そこで本研究では、観測、モデル、データ同化、理論を駆使して、金星の大気波動の実態を明らかにすることを目的とする。

**方法:** 我々は、これまでに地球シミュレータ上の金星大気大循環モデル (AFES-Venus) および世界初のデータ同化システム (ALEDAS-V) を開発してきた。本研究では、①あかつき観測データを AFES-Venus に同化することで、あかつきで観測される様々な時空間スケールの金星大気波動を再現、②AFES-Venus 単体での高解像度計算によって、より細かいスケールの波動現象の再現を試み、③これら数値モデルで得られた波動について、3 次元構造や働きについての解析を行い、理論的な解釈を行う。④また、国内外の金星大気大循環モデルで得られる波動についても、その発生条件や構造の違い等を本モデルの結果と比較する。⑤さらに、波動を疑似観測データとして同化する実験 (OSSEs) を行い、波動の同化で再現できる新規観測の立案を行う。

**結果:** 2023 年度は、あかつき中間赤外面像から得られる温度の同化を試行した結果、熱潮汐波の位相が改善された。また、AFES-Venus 単体で再現されるスーパーローテーションについて、解像度を変えて水平粘性依存性を調べた結果、水平粘性に依存しないパラメータ領域を見出した(成果報告②)。さらに、あかつき紫外画像を想定した観測システムシミュレーション実験 (OSSEs) を実施し、ロスビー波の再現に向けた観測条件を探索した。衛星間電波掩蔽を用いたコールドカラーの再現可能性に関する OSSEs の結果を論文化した(成果報告③)。さらに、大気大循環モデルの改良として、加熱や安定度分布を修正し、熱潮汐波や短周期波動の再現性が向上し、これらの解析も進行中である。

**考察:** 2023 年度に得られた結果から、あかつきの温度同化は風速と異なり、基本場を大きく変更する可能性があることがわかった。これは観測とモデル間の平均温度に大きなバイアスが存在することに起因している。このため、2024 年度には、温度場のバイアス補正を行うことや、中間赤外面像の射出角に応じて同化する高度を変えるなどの方法を検討している。また、ロスビー波とケルビン波のカップリングによる結合不安定の理論的解釈が必要である。特に Venus Express やあかつきによる長期観測により、雲層のアルベドやスーパーローテーションの長期的な変動が報告されており、3 次元の波動の時空間変動が深く関わる可能性が示唆されている。このため、これまでに得られている 3 次元の波動の励起メカニズムの解明が望まれる。またモデル間比較により、金星大気波動の普遍性について、今後は理解を深めていかなければならないと考える。

**研究成果報告:** ①Fujişawa, Y., N. Sugimoto 他 6 名, Evaluation of new radio occultation observations among small satellites at Venus by data assimilation, *Icarus*, Vol. 402, (2023), 115728, 10pp.

②Sugimoto, N., Y. Fujişawa, N. Komori 他 3 名, Super-rotation independent of horizontal diffusion reproduced in a Venus GCM, *Earth, Planets and Space*, Vol. 75, (2023), 44.

**研究組織:** 杉本憲彦 (研究代表者)、藤澤由貴子、小守信正: 慶應義塾大学  
大貫陽平 (所内世話人)、山本勝: 九州大学応用力学研究所

**Nonlinear energy transfer within the oceanic internal wave field (2023S1-IC-2)**

Applicant: Wei Yang (Tianjin University)

**Abstract**

To investigate the nonlinear energy transfer within internal wave fields, we continued to analyze the observations and carry out numerical simulations during the last year. We have performed bispectral analysis to determine the direction of energy transfer in vertical wavenumber space. The results showed similarities with the in-situ oceanic observations of the previous study during this project. A new interesting result we obtained during the project is that we found the interaction mechanism may resemble the classical wave-mean flow interaction mechanism. However, here the mean flow oscillates with near-inertial frequency. This is an interesting mechanism and awaits further investigation in depth. We suspect that this mechanism may be important in understanding the oceanic internal waves interactions and play an essential role in the real ocean.

**1. Purpose**

Tropical cyclones (TCs) represent the most extreme atmospheric disturbances passing over the ocean which can excite intense oceanic responses from both thermal and dynamic views. These responses are in multiple forms, such as significant surface cooling, surface waves, geostrophically balanced motions, intense turbulence and mixing, and internal waves at various frequencies. A more comprehensive understanding of the oceanic wave responses is required which is crucial for the understanding of energy pathways from TC forcing to ocean interior mixing.

The possible energy exchange and interactions between internal waves at different frequencies further added to the difficulty in understanding the oceanic responses to passing TC. Based on moored velocity measurements in the northern Gulf of Mexico, Jing et al. (2015) observed the energy transfer from near-inertial to superinertial internal waves after the passing of a TC which was further demonstrated to play an important role in elevating the superinertial shear variance. The understanding of the energy exchange is crucial for understanding how the TC distributes their energy and feeds mixing in the ocean interior. However, observations so far remain limited in picturing the problem, and we are still unclear how the internal waves at super-inertial frequencies after TC can be fueled.

The East China Sea (ECS) is a midlatitude marginal ocean with a long continental shelf slope in the northeast-southwest direction. It is located adjacent to the western North Pacific Ocean which is the most active tropical cyclone basin in the global oceans. Furthermore, this region is also characterized by the strong west boundary current, Kuroshio, and rich internal wave fields such as semidiurnal internal tides and internal solitary waves which together form quite complicated dynamic fields (Min et al., 2023). Based on the measurements from a mooring station at the shelf slope northeast of the Taiwan island, we aim to understand oceanic wave responses to a passing TC at near-, and super-inertial frequency ranges and investigated the associated dynamic mechanisms.

**2. Methods**

The main observation data used here was acquired at a mooring station at the ECS from Aug. 27 to Oct. 28, 2013. Horizontal velocities were measured by two acoustic Doppler current profilers

(ADCPs 75-kHz Long Ranger, Teledyne-RD Instruments), which were deployed at 445 and 455 m with one looking upward and the other looking downward, having a temporal resolution of 5 minutes and vertical resolution of 8 m. Valid velocity measurements covered a depth range of 50 – 710 m. Due to the separation between the upward-looking and downward-looking ADCP sensors, velocity measurements had a gap in the mid-water column which was supplemented by linearized interpolation. Measurements of temperature across the water column were sampled by 24 temperature-depth sensors (TD, SBE37) and 7 conductivity-temperature-depth sensors (CTD, SBE37).

Following Sun and Pinkel (2012), we calculated the energy transfer rate from near-inertial to high-frequency internal waves following

$$\mathcal{G} = -\sum \langle u'_i w' \frac{\partial u_i}{\partial z} \rangle, i = 1, 2 \quad (1)$$

where the angle bracket  $\langle \rangle$  represents time averaging,  $u'_i$ ,  $w'$  are the horizontal and vertical velocities associated with HFIWs, respectively,  $\frac{\partial u_i}{\partial z}$  is the velocity shear of low-frequency internal waves, subscript  $i = 1, 2$  stands for the zonal and meridional components, and  $\Sigma$  represents the summation over the subscript  $i = 1, 2$ .  $u'_i$ , and  $w'$  were highpass filtered above 6 cpd. The vertical shears ( $\frac{\partial u_i}{\partial z}$ ) here were bandpass filtered at a frequency range of  $(0.8-1.3)\omega_f$ .  $w'$  was derived from the vertical motion of isotherms which originally had 1-min temporal resolution and was discrete in vertical space. To calculate  $\mathcal{G}$ , we averaged the  $w'$  into 5-min segments and interpolated them to the ADCP bins. Furthermore, the semi-Lagrangian reference frame which was obtained by referencing measurements to isotherms was used in the calculation (Yang et al., 2022).

### 3. Results and discussion

#### 3.1 Occurrence of high-frequency internal waves after TC Fitow

The wavelet spectra of the depth-averaged vertical velocity showed that in addition to the typical near-inertial response after TC, the other pronounced response was located at the high-frequency range appearing immediately after TC Fitow at 18:00, Oct. 7. This high-frequency response had a period of 0.2 – 0.8 h lasting ~ 8 hours.

A close examination of the calculated rms vertical velocity at high-frequency bands ( $\sigma_w$ ) showed that the HFIW appeared in a regular semidiurnal ( $M_2$ ) period before the approaching of TC Fitow (vertical gray dashed lines in Fig. 1d). Previous studies showed that the HFIWs at the study area were ubiquitous, having multiple generation sites and traveling in different directions (Duda et al., 2013). These HFIWs can be generated by various mechanisms such as the local tide-topography interactions, and disintegration of internal tides remotely generated over I-Lan Ridge (Min et al., 2023). The regular semidiurnal occurrence before TC Fitow also indicated the tidal origin of the HFIWs. The intense HFIW packet emerging at 18:00, Oct. 7, 30 hours after the pass of the TC center, was different from the typical HFIWs in the study area. The calculated  $\sigma_w$  showed that the intense HFIW event did not follow the regular semidiurnal occurrence before TC Fitow (Fig. 1d).

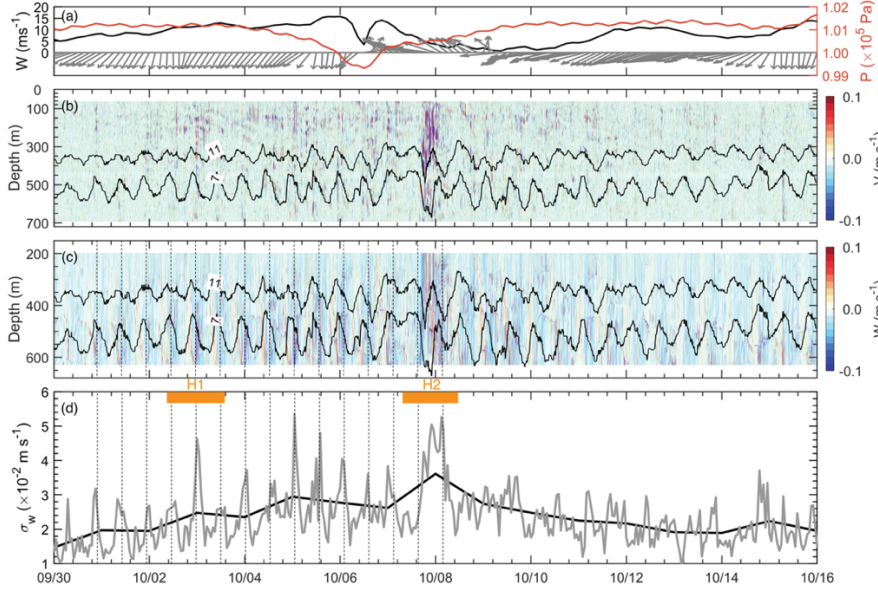


Fig. 1. (a) Time series of the wind speed (black line), wind direction (gray arrows), and air pressure (red line) at the mooring station. (b) and (c) are the depth-time maps of highpass-filtered ( $\omega > 24$  cpd) meridional and vertical velocities, respectively. The contoured lines are isotherms of 7 and 11  $^{\circ}\text{C}$ . (d) The rms vertical velocity ( $\sigma_w$ ) at high-frequency bands ( $\omega > 24$  cpd). The gray and black lines represent the calculated values in 1- and 24-hr intervals, respectively. The vertical dashed lines in (c) and (d) denote a regular  $M_2$ -period separation.

### 3.2 Energy transfer properties

With this limited dataset, it was not possible to establish the exact nature of the intense HFIW after TC Fitow. We next seek to understand the plausible energy transfer between the HFIWs and background internal waves. How the HFIWs were energized by NIWs after their generation is of interest here.

The calculated  $\mathcal{G}$  showed that energy was efficiently transferred from near-inertial to high-frequency bands of the internal waves (overall positive values in Fig. 2). Along with the appearance of intense HFIWs after TC,  $\mathcal{G}$  was elevated by one order of magnitude with the depth-averaged approaching  $2 \times 10^{-6} \text{ W kg}^{-1}$ . Besides the temporal variation, the calculated  $\mathcal{G}$  also showed an interesting structure of horizontal layers with vertical scales of  $\sim 100$  m (Fig. 2b). This was largely related to the vertical structure of NIWs. Those horizontal layers in  $\mathcal{G}$  disappeared if we applied a much broader bandpass-filtering frequency range to the vertical velocity shear ( $0.6 < \omega < 3$  cpd instead of  $0.8-1.3\omega_f$ ). However, the averaged  $\mathcal{G}$  did not vary a lot demonstrating the dominant role of NIWs in the energy transfer.

Based on measurements taken in the nearfield of the tidal conversion site near Kaena Ridge, Hawaii, and near the ECS shelf break, previous studies have also documented the energy transfer from NIWs to HFIW which had similar average values at the order of  $1 \times 10^{-7} \text{ W kg}^{-1}$  (Sun and Pinkel, 2012; Yang et al., 2022). Observations in the open ocean revealed much less averaged energy transfer which is almost two orders smaller ( $3.7 \times 10^{-9} \text{ W kg}^{-1}$ ) (Chen et al., 2023). The calculated  $\mathcal{G}$  after passage of TC Fitow along with the appearance of intense HFIWs was much larger than those previous estimations. This demonstrated efficient energy transfer from NIWs to HFIW. The efficient energy transfer can aid the growth of HFIW and play a key role in redistributing the TC-injected energy in the ocean interior.

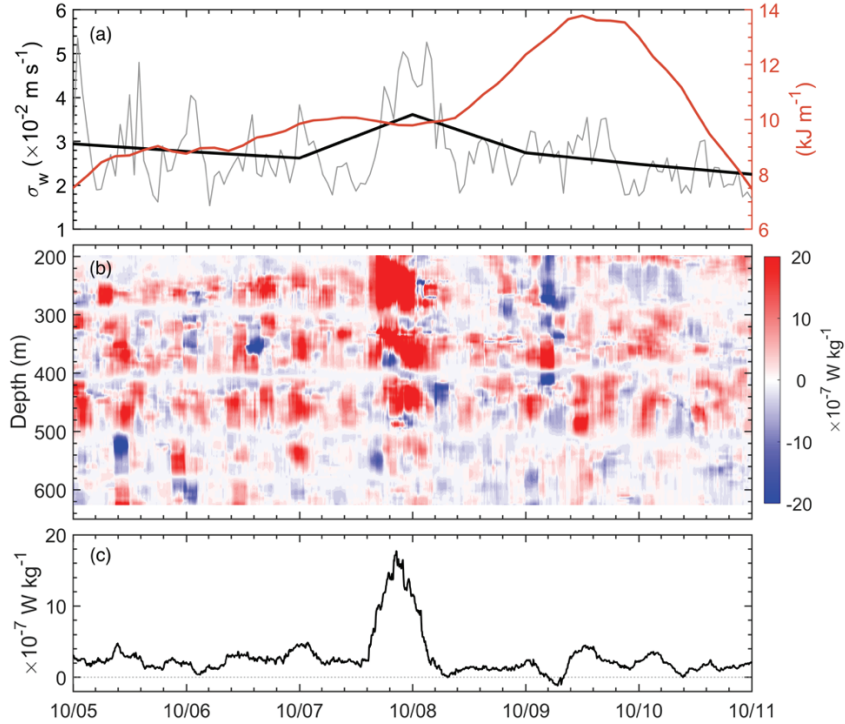


Fig. 2. (a) Time series of the rms vertical velocity ( $\sigma_w$ ) at high-frequency bands in 1- (gray line) and 24- (black line) hour intervals. The red line represents the depth-integrated HKE of NIWs. (b) and (c) are the energy transfer rate from NIWs to HFIWs and the corresponding depth-averaged values, respectively.

#### 4. Future work

Although we have identified nonlinear energy transfer from NIWs to HFIWs from the observation data in the East China Sea, the detailed mechanism of this interesting process remains to be explored. From a mathematical viewpoint, the temporal scale separation between slowly varying NIWs and rapidly oscillating HFIWs enables the use of wave-mean flow interaction theory. In this framework, the propagating and amplification of HFIWs in the NIWs field are represented by the set of ray-tracing equations, and the feedback to NIWs can be evaluated by the radiation stress computable from the pseudo-momentum flux. At the end of this year, we have derived a suitable model equation system describing this mutual-interaction process. Preliminary numerical simulations were carried out to exhibit the decay of NIWs through the radiation of HFIWs over a corrugating sea floor (Fig. 3). A thorough analysis of the simulation results and the investigation of parameter dependence are planned for the next year.

#### References

- Duda, T. F., A. E. Newhall, G. Gawarkiewicz, M. J. Caruso, H. C. Graber, Y. J. Yang, and S. Jan, 2013: Significant internal waves and internal tides measured northeast of Taiwan. *J. Mar. Res.*, **71**, 47–82.
- Jing, Z., P. Chang, S. F. Dimarco, and L. Wu, 2015: Role of near-inertial internal waves in subthermocline diapycnal mixing in the northern Gulf of Mexico. *J. Phys. Oceanogr.*, **45**, 3137–3154.
- Min, W., Q. Li, Z. Xu et al., 2023: High-resolution, non-hydrostatic simulation of internal tides and solitary waves in the southern East China Sea. *Ocean Model.* **181**, 102141.
- Sun, O. M., and R. Pinkel, 2012: Energy transfer from high-shear, low-frequency internal waves to high-frequency waves near Kaena Ridge, Hawaii. *J. Phys. Oceanogr.*, **42**, 1524–1547.

Yang, W., H. Wei, and L. Zhao, 2022: Energy transfer from PSI-generated M1 subharmonic waves to high-frequency internal waves. *Geophys. Res. Lett.*, **49**, e2021GL095618.

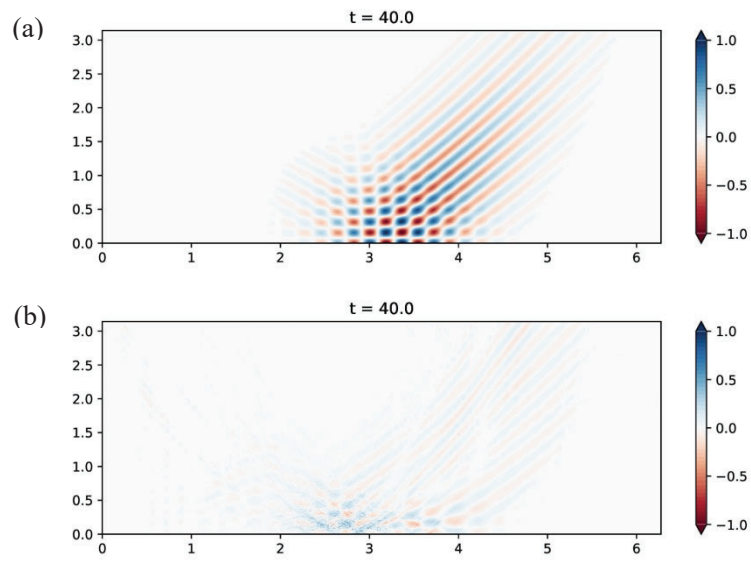


Fig. 3. Snapshots of the zonal velocity of near-inertial waves in numerical simulations. A near-inertial wave packet is reflected over (a) flat and (b) corrugating sea floors.

RIAM host: Yohei Onuki

## Quasi-resonance phenomena in geophysical waves

APPLICANT: Antoine VENAILLE, (ENS de Lyon, France)

**Reminder: the scientific context of the proposal**

This project is motivated by geophysical phenomena. We advocate the fruitful exchange of ideas between geophysical fluid dynamics and other fields of physics. We identified several geophysical wave problems that can be tackled by using the Wigner-Weyl transform and related techniques.-

**Scientific questions addressed in 2022**

The first question we asked was « can be used ray tracing and semi-classical analysis to understand the topological origin of equatorial waves ». *This project emerged building on previous work by A. Venaille on one side, and of Y. Onuki on the other side. Thanks to the RIAM collaborative project, combining our different knowledge on this topic allowed us to obtain a new result which may have an impact beyond geophysical fluid dynamics, see abstract below.*

**Scientific questions addressed in 2023**

In recent years, there has been a strong interest in Lyon for the application of tools from topology to the physics of waves. The theoretical framework involves Wigner-Weyl calculus and is very relevant to this collaborative research project. Together with Pierre Delplace, we started a new line of research aiming at proving bulk-edge correspondence for fluids, a cornerstone of topological wave physics. We also generalized the flow spectral approach to shear stratified flow on the equatorial beta plane with application to the planetary atmosphere.

*This part was led by Yohei Onuki, and used the expertise in Lyon on topological wave physics.*

**The concrete outcome of the project**

**[1] 2023 Venaille Onuki** Perez Leclerc, *From ray tracing to waves of topological origin in continuous media*, <https://arxiv.org/abs/2207.01479>. *This paper is published in SciPost, which features an open review process; one of the reviewers qualifying the work as « an illuminating tour-de-force ».*

*Abstract:* Here, by applying ray tracing machinery to the paradigmatic example of equatorial shallow water waves, we propose a physical interpretation of the bulk-edge correspondence, a cornerstone of topological wave physics.

**[2] 2023 Onuki Venaille** Delplace, *Bulk-edge correspondence recovered in incompressible continuous media*, <https://arxiv.org/abs/2311.18249>. *This paper will be submitted to Physical Review Research.*

*Abstract:* In continuous media, the bulk-edge correspondence can be violated, resulting in weak topological protection of chiral edge states. Here, we propose a strategy to reestablish strong bulk-edge correspondence in incompressible continuous media.

**Conference presentations**

- [1] Venaille, Wave topology in fluids, Seminar at LOMA Marseille, Dec. 19, 2023.
- [2] Venaille, Wave topology in fluids, Seminar at Grenoble, Nov. 27, 2023.
- [3] Venaille, Wave topology in fluids, Seminar at Cambridge, Oct. 5, 2023.
- [4] Venaille, Wave topology in fluids, Winter School NORDITA Stockholm, Jan. 20-26, 2023.
- [5] Venaille, Wave topology in fluids, Summer School GRENOBLE, Jun. 6-13, 2023.

RIAM host: Yohei ONUKI

## Small-scale instabilities in rotating and stratified fluids

Professor Manikandan Mathur  
Department of Aerospace Engineering  
Indian Institute of Technology Madras, Chennai, India.

Internal waves play a significant role in promoting vertical mixing in the ocean, and hence contributing to the global circulation and energy budget. In this joint research, we study the evolution of small-amplitude and short-wavelength instabilities in internal waves using a local stability method and Direct Numerical Simulations. The investigation is motivated by the dynamics of inertial-gravity waves in the ocean, which are well-described within a Cartesian geometry for processes that do not extend over vast latitudinal or longitudinal ranges. The plots of growth rates were made in the perturbation space for the base flow inertia-gravity wave parameters ( $\omega/N, \omega/f$  and  $A$ ), where  $\omega$  is the frequency of the base wave,  $N$  is the buoyancy frequency,  $f$  is the Coriolis parameter and  $A$  is the non-dimensional amplitude. Figure 1 shows the growth rates for  $\omega/N = 0.25, A = 1$  and  $\omega/f = 1.5, 2.1, 5$ . Clear instability bands are observed on the perturbation parameter space. For a given base inertial-gravity wave, the dominant instability has also been identified for the perturbations for which the growth rate is maximum. These results are being prepared for a research article in the Journal of Fluid Mechanics. Direct numerical Simulations of turbulence and mixing induced by short-wavelength instabilities in inertia-gravity waves have been discussed and planned to be performed in 2024.

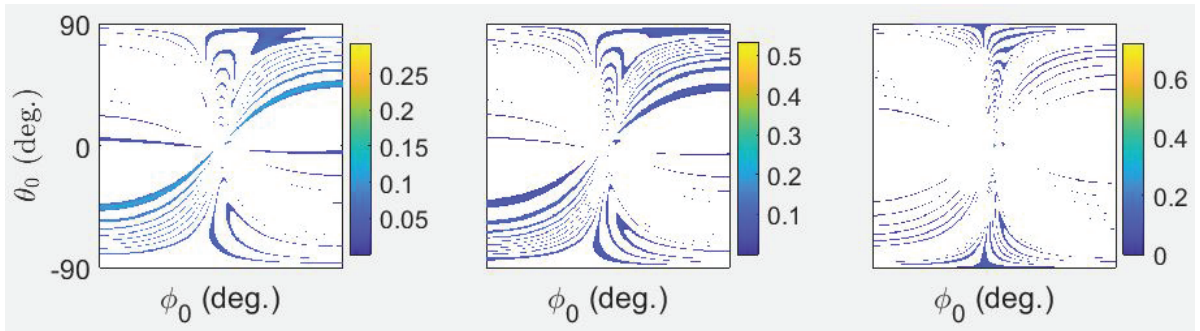


FIG. 1: Growth rate ( $\sigma$ ) non dimensionalized by  $\omega$ , as a function of perturbation wave vector orientations  $\phi_0$  (deg.) and  $\theta_0$  (deg.) for  $\omega/f = 1.5, 2.1, 5$  (column-wise) and  $A = 1$ , with  $\omega/N = 0.025$ .

Local stability analysis was also conducted in the limit of internal waves with rotation and no stratification, namely inertial waves. At sufficiently small am-

plitude, three-dimensional parametric subharmonic instability (PSI) is the only instability mechanism. As the amplitude is increased, theoretical PSI estimates become less relevant in describing the instability characteristics, and the dominant instability transitions to two-dimensional shear-aligned instability, which is shown to be driven by third-order resonance. The dominant instability characteristics are shown in figure 2. The results of this work have been accepted for publication in the Journal of Fluid Mechanics. The discussions with Dr. Yohei Onuki through the RIAM joint research program have been acknowledged in the paper.

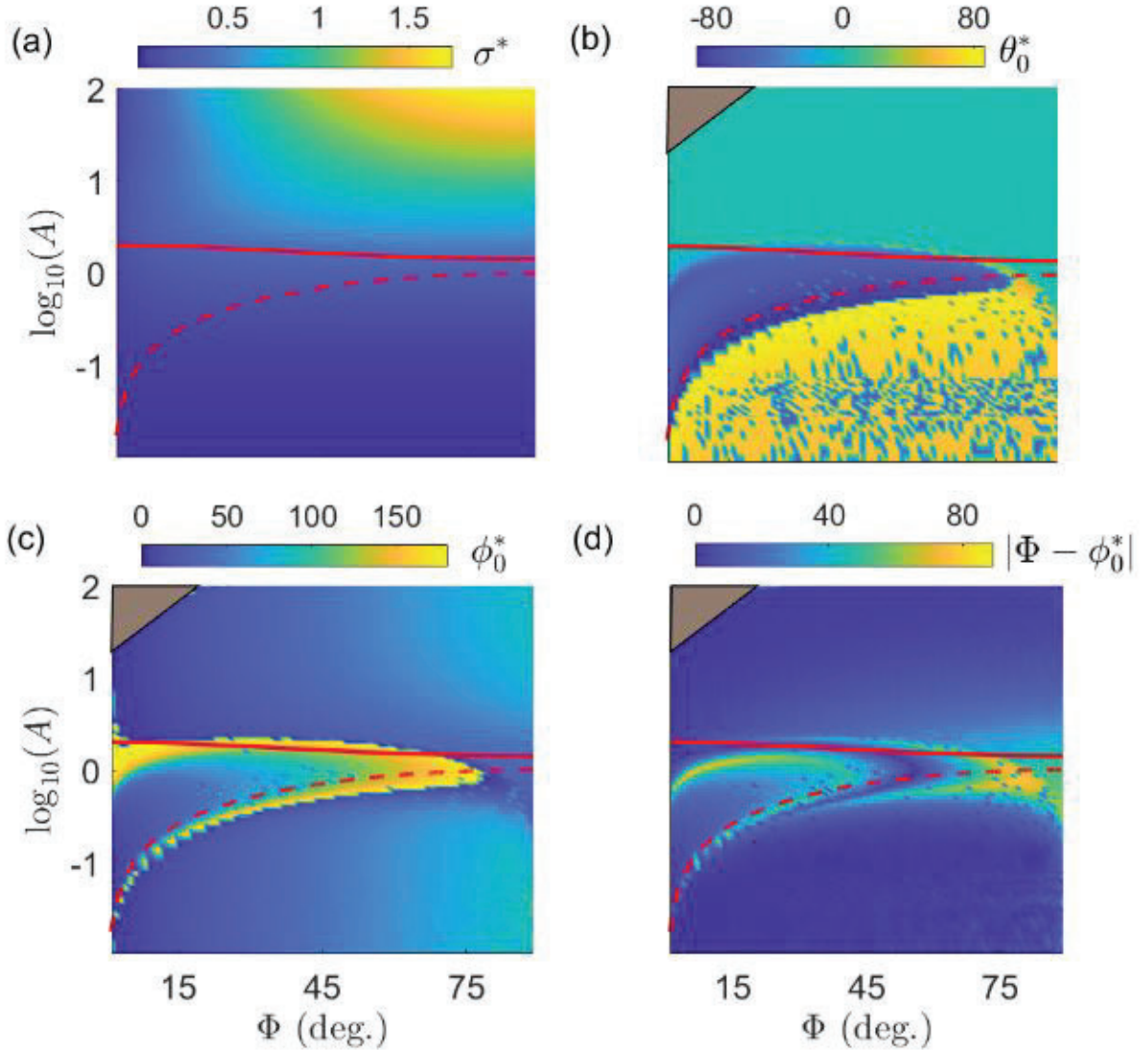


FIG. 2: Dominant instability diagram for an inertial wave. (a) Maximum growth rate  $\sigma^*$  as a function of  $\Phi$  and  $A$ , and the corresponding (b)  $\theta_0^*$  and (c)  $\phi_0^*$  at which the maximum growth rate occurs. (d) Angle between the inertial wave vector and the most unstable perturbation wave vector,  $|\Phi - \phi_0^*|$ , as a function of  $\Phi$  and  $A$ .

Professor Manikandan Mathur had a successful visit to RIAM, Kyushu University from 23rd September to 5th October, 2023, and held several collaborative research discussions with Dr. Yohei Onuki and colleagues. The visit started with participation in The Oceanographic Society of Japan, Fall Meeting (9/24-28, 2023) 2023 Fall Meeting of the Oceanographic Society of Japan was held at Kyoto University. Research discussions were focused on short-wavelength instabilities in inertia-gravity waves, and a clear roadmap for theoretical calculations has been developed. Professor Manikandan Mathur gave a talk on “Instabilities in internal gravity waves” and also held discussions with several researchers at RIAM. Dr. Shinichiro Kida, RIAM, Kyushu University was hosted for an online seminar on “River-Ocean Interaction of the Ganges-Brahmaputra-Meghna Delta” at the Geophysical Flows Lab, IIT Madras. Some photos from Manikandan Mathur’s visit to RIAM are included below.

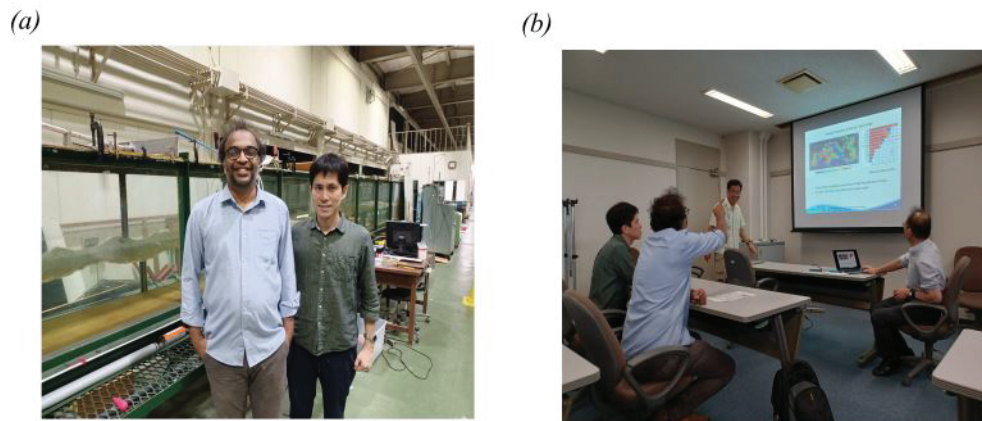


FIG. 3: (a) Professor Manikandan Mathur with Prof Yohei Onuki at an experimental waves facility in RIAM, Kyushu University. (b) Brainstorming sessions on the interaction between internal waves and Kuroshio current.

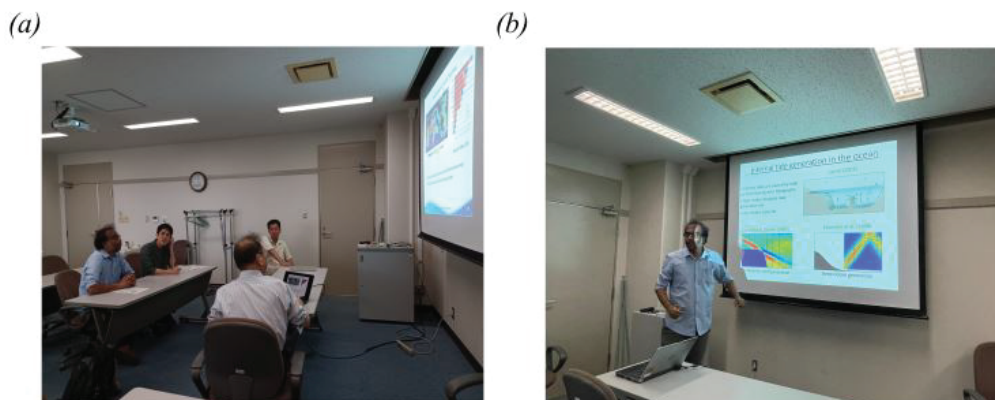


FIG. 4: (a) Discussions at RIAM, Kyushu University (b) Professor Manikandan Mathur presenting a seminar at RIAM, Kyushu University.

## Triadic resonant instability of internal gravity waves in a stratified shear flow

APPLICANT: Anubhab Roy, (IIT Madras, India)

**Summary:**

In this work, we study the stability of an internal gravity wave (IGW) mode in a 2D, inviscid, uniformly stratified, linear shear flow confined between two walls. Assuming the reference frame to be moving with the phase speed of the IGW mode, and a small amplitude, we evaluate the vertical structure of the IGW mode. The stability of this mode, then, is studied using Floquet theory. The growth rates and the corresponding vertical structures of the perturbation variables can be obtained by solving a generalized eigenvalue problem for the two discrete interacting perturbation modes. At resonance, the frequencies of both modes should be equal. An asymptotic calculation is done with a small detuning between the two frequencies to obtain the growth rates near the resonant interactions. The growth rates, thus obtained, are compared with the solution by solving the generalized eigenvalue problem numerically.

**Theoretical model:**

We consider a base field as a stably stratified fluid flow superimposed with a stationary internal gravity wave with rigid top and bottom boundary conditions. The following set of equations governs the linear stability of this system to infinitesimal perturbation:

$$\frac{\partial \nabla^2 \psi'}{\partial t} + J(\tilde{\psi}_B, \nabla^2 \psi') + J(\psi', \nabla^2 \tilde{\psi}_B) = -\frac{g}{\rho^*} \frac{\partial \rho'}{\partial x}$$

$$\frac{\partial \rho'}{\partial t} + J(\tilde{\psi}_B, \rho') + J(\psi', \rho_B) = 0$$

Here,  $\psi$  and  $\rho$  represent the stream function and density, respectively. A symbol with a subscript B denotes the base field component, and that with a prime denotes a perturbation.

Assuming the spatial periodicity of the base wave field, we apply the Floquet theory to expand the disturbance as the sum of a Fourier series and derive a generalized eigenvalue equation determining the instability growth rate. We also apply the asymptotic analysis to obtain the analytical expression of the growth rate and compare it with numerical solutions (Figure).

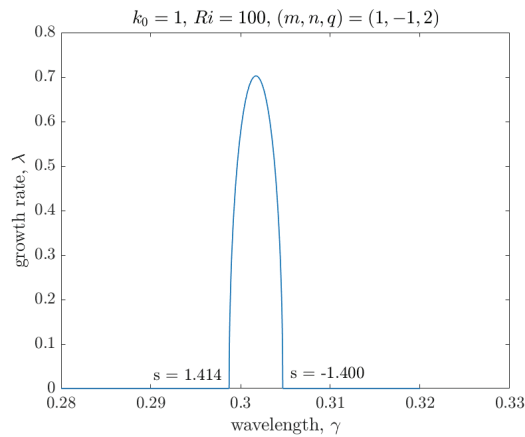


**Figure.** Instability growth rate  $\lambda$ , as a function of the disturbance wavelength  $\gamma$ . The amplitude and width of the unstable region agree well between the analytical and numerical solutions.

**Publications:**

- Kadam, Y., Patibandla, R., & Roy, A. (2023). Wind-generated waves on a water layer of finite depth. *Journal of Fluid Mechanics*, 967, A12.
- Patibandla, R., Basak, S., Dasgupta, R., & Roy, A. (2023). Surface and internal gravity waves on a viscous liquid layer: Initial-value problems. *International Journal of Multiphase Flow*, 169, 104592.

**Conference presentations:**

- Patibandla, R., Mathur, M., & Roy, A. Triadic resonances in internal wave modes with background shear. *European Geosciences Union (EGU) 2023*, Vienna, Austria, April 2023.

RIAM host: Yohei ONUKI